CHANGE DETECTION UNDER UNCERTAINTY: MODELING THE SPATIAL VARIATION OF ERRORS

Sotirios Koukoulas

Dept. of Geography. Spatial Analysis, GIS and Remote Sensing Lab.
University of the Aegean
Mytilene 81100, Greece
skouk@geo.aegean.gr
www.aegean.gr/geography

Commission VIII/8

KEY WORDS: Land Cover, Change Detection, Error, Modelling, Spatial, Statistics, GIS

ABSTRACT:

This research focuses on modeling the spatial variation of errors in a land cover map and in the detection of changes when local uncertainties are identified. The motivation for this research stems from the fact that although a plethora of classification accuracy indices exists, most of them are global measures, such as the percentage correct and kappa index which are being the dominant measures so far. There is certainly a need to know the spatial distribution of errors in order to take informed decisions for further research and better interpretation of the results. The methodology that was followed, initially focused to land cover mapping and change detection mapping, for land use changes that have taken place since 1975. The latter was achieved by devising a simple and operational rule-based approach to map land cover changes, based on the classification of Landsat imagery (MSS for 1975 and TM5 for 1990, 1999, 2007) and the conceptual analysis of the information regarding change detection. The use of ancillary GIS data such as a Digital Elevation Model, existing thematic maps and the knowledge of the island's vegetation dynamics, formed the basis for setting the rules (e.g. impossible changes, valid transitions) for the post-processing of the classified images that led to a more accurate assessment and mapping of land cover changes.Consequently, a model-based approach to estimate local uncertainties is proposed by using independent ground truth samples and GAM models to estimate the probability of error occurrence in the study area. Change detection maps were subsequently cross-tabulated with error maps in order to provide information on the reliability of the change estimates.
The results can be used in various ways. Firstly, as an iterative classification process corrected by independent ground truth samples, taken at the areas with low accuracy. Secondly, the analyst can proceed to use the enhanced change detection maps, making informed decisions and incorporating uncertainties in future modeling.

1 INTRODUCTION

Land cover map accuracy measures are global measures and at best they provide information at class level. Quite a few indices for accuracy assessment have been developed in the past with percentage correct and kappa index being the dominant measures so far. The importance of accuracy assessment for each land category has long being recognized and each of these indices have been extended to report accuracies for each class.

Error matrices do offer a lot of information for the classification accuracy reporting both errors of omission and errors of commission for each class. However not all of this information is passed to the indices of accuracy. In fact almost all of the indices proposed and used are ignoring errors of commission. Yet these errors are as important as the omission errors. Koukoulas and Blackburn (2001) have offered an overall index (CSI), group and individual class indices that do take into account both types of errors (omissions and commissions). However, this is a problem of spatial distribution of errors. In order to tackle efficiently the estimation of uncertainty in a land cover map we need to know the probability of each pixel being correctly classified based on independent ground truth samples.

Not knowing the spatial distribution of errors of commission and errors of omission is a major issue for reporting land cover statistics and furthermore land cover change estimates. This is also important for the estimation of error propagation in models that use land cover maps as inputs, e.g. erosion models.

Certainly,there is a need for local measures of uncertainty in order to have a clearer picture of what we are mapping. Local indices of map quality based on the classification probabilities for each class were produced in the past by Kyriakidis and Dungan (2001) using indicator kriging modeling. Other interesting approaches in modeling errors for remotely sensed data can be found in Wang and Howarth (1993) who studied the uncertainties involved in class modeling (training) and boundary generation (boundary pixel allocation), de Bruin (2000) who worked on the prediction of the areal extent of land-cover types using Geostatistics, Crosetto et al. (2001) who worked on uncertainty propagation on remotely sensed data and van Oort (2007) where his approach provides new insights on the change detection error matrix. This study is using a model-based approach to local uncertainty estimation by using independent ground truth samples and GAM models to estimate the probability of a pixel being correctly classified and the spatial variation of errors on the map.

2 METHODOLOGY

The methods used in this project are detailed below. First, the study area is described as well as the setup of the data for the spatial analysis followed. Consequently, the theoretical background of non parametric binary regression and Generalized Additive Models are described and applied in order to test the spatial variation of errors in each classified map. An approach for change detection under uncertainty is also described.

2.1 Study area and data description

The study area is the island of Lesvos in Greece, which over the last three decades has experienced significant and complex land cover/use changes despite being far from the mainland and without intense tourist growth (Gatsis et al., 2006; Giourga et al., 2008).

Four satellite images, a Landsat MSS scene (July 1975, 4 bands, nominal pixel size 59m), and three Landsat 5 TM scenes (June 1990, July 1999, August 2007, 7 bands, nominal pixel size: 30m), were employed for identifying land cover and land cover changes in the island of Lesvos. Additional ground truth data were derived from orthorectified aerial photographs at a scale of 1:40.000, dating 1960,1995, Quickbird imagery 2001, Google Earth data for 2007 and GPS field data for 2001 and 2007.

2.2 Land cover mapping and change detection

Geometric correction of the images was performed using 2nd order polynomials and nearest-neighbor resampling with a RMS smaller than one pixel. The four scenes were referenced to a common projection (EGSA 87). The four images were classified using the Maximum likelihood classification rule with randomly selected samples for each land cover class. Initially eight (8) land cover classes were used; bare land, garrigue (phryganic vegetation including natural pastures), maquis vegetation (open and dense), pine forest, broadleaved forest, olive cultivations, urban areas (including quarries) and water bodies. Some types of land cover such as specific arable crops (other crops), marsh and saltworks were excluded from the classification process due to their high spectral variability and confusion with other classes. These classes were added later, during the rule-based approach. The samples for the MSS image classification (1975) were collected from orthophotos, dating from 1960 as there was no availability of aerial photographs nearer 1975. The samples were distributed randomly within the land cover zones of a (Forestry Service) vegetation map dating from 1960. This map was a useful guide especially in areas where identification of land cover types was difficult (e.g. between maquis and olive trees). Manual editing of the samples ensured the match of sampled land types between the orthophotos and the MSS image. The samples for the 1990 Landsat TM5 image were collected from the 1995 aerial photographs, for the 1999 Landsat TM5 were collected from the Quickbird imagery (2001) and land surveys using GPS (year 2003). Despite the thorough sampling framework, the produced thematic maps of land cover/use alone were not suitable for change detection. For the year 1975, the poor spatial and spectral resolution of Landsat MSS produced classifications of low accuracies (58%). In the early years of remote sensing these accuracies were considered adequate. Currently, the challenge is to improve on this (using MSS imagery) and subsequently use the results for change detection purposes. The significance of the latter is obvious if we consider the large existing archive of MSS data (mostly available for free) that could provide useful insights to the status of land cover 30-35 years ago. A rule-based approach was used, combined with manual editing which allowed us to produce classified images with accuracies of 88.5% for the 1975 image. The rule-based enhancement did improve accuracies of Landsat TM classified products, which were also low. The lower accuracies of Landsat TM are due to the higher spectral confusion among three classes, namely olive trees, maquis and garrigue that cover a large part of the island (approximately 75%). Following the same approach (as for MSS) for Landsat TM classified images the final classification reached 93% accuracy for the 1990 image, 95.6% accuracy for the 1999 image and 90.3% accuracy for the 2007 image.

Rule-based enhancement of the classified images that was mentioned above, involved corrections with regard to topography of the area (e.g. Olive cultivations found above 350m for a certain zone of the study area were reclassified to maquis vegetation (spectral and texture similar class), correction of urban areas where they we confused with bare land based on ancillary GIS data and identification of false changes. The latter involved identification of erroneous changes using field and ecological knowledge (e.g. changes that are impossible to happen in the time span studied) and correction of the classified images focusing on the areas where erroneous changes occurred. The latter was implemented using all four images and looking for patterns of the type 'Pine forest-other-Pine forest-Pine forest' or obvious variability in the changes, such as 'Pine forest-Olives-Pine Forest-Olives'. More details on the classification procedure and parts of rule based approach can be found in Gatsis et al. (2006, 2007); Gatsis and Koukoulas (2009). Note that the papers above did not use all four images simultaneously - this was part of the current work.

2.3 Spatial variation of the errors

Given an initial set of sample locations the objective is to derive accuracy measures on the land cover maps produced by classification (or otherwise).

Although the initial set was chosen randomly, each subset of correct or erroneously classified locations (pixels) might exhibit a particular pattern making decisions based on the corresponding land cover map problematic. More importantly land cover change maps would be non-uniformly affected making interpretation and conclusions unreliable. If the errors are randomly distributed and their total percentage is low then we can accept a land cover map for further processing, otherwise we should map the pattern of errors and take it into account into further processing or into designing new sampling layouts for classification improvement.

In order to model the local variation of error in a land cover map given only the position as explanatory variable we assume that we have a set of locations $X_i \in L$, here each pixel is a location and L is our study area. The objective is to model the probability of each location (pixel) to be correctly classified. A sample of N such locations Z_i with i=1...N, is selected randomly from the land cover map and tested against ground truth data derived from the interpretation of aerial orthophotographs and fieldwork for all the years (fieldwork refers only to the last two dates 1999 and 2007). A number n_1 from these samples was labeled as correct (1) and $n_0 = N - n_1$ were labeled as errors (0).

In order to map the pattern of errors we can use first Kernel density estimation for each group of locations and then we evaluate their ratio. Each step is described in the following subsections.

2.3.1 Kernel density estimation: Kernel estimation was originally developed to obtain a smooth histogram from an observed sample and it has since been adopted to estimate intensity of an observed pattern using a function known as kernel (Silverman, 1986; Bailey and Gatrell, 1995). The kernel function can be conceptualized as a moving function usually in the shape of a circle or square that is applied over a fine grid of locations in the area of interest and visits each point in this fine grid. Distances to each observed event that lie within the region of influence (e.g. within a radius r for a circle) are measured and contribute to the intensity estimate of the origin according to how close they are to the origin. Again here the problem of choosing the right radius (if it is a circle) exists, as a very large r will obscure local features and make the area look flat and a very small r will result in a spiky surface. As a solution methods have been proposed to adjust (and to

optimize) the radius of the kernel function for regions with different density in order to improve the intensity estimate (see Bailey and Gatrell, 1995 for more details of the kernel function). A two dimensional kernel density estimate at location $Z = (x_0, y_0)$ is defined as:

$$\tilde{\lambda}(Z_0) = \frac{1}{Nr_xr_y} \sum_{i=1}^{N} \left\{ kern\left(\frac{x_0 - x_i}{r_x}\right) kern\left(\frac{y_0 - y_i}{r_y}\right) \right\} \tag{1}$$

where r_x and r_y are the bandwidths in x and y directions. Usually we use symmetric kernels and the bandwidth is equal to r for both directions. $kern()$ is known as kernel and the researcher can choose from a list of symmetrical to the origin bivariate probability density function. For this study the bivariate normal probability density function was used as kernel, with r equal to 3km, estimating the function for a grid of locations $S = (x, y)$ and creating the overall intensity surface.

Many researchers use the terms density and intensity interchangeably because these two functions differ only by a constant of proportionality. Density function in our case defines the probability of observing an erroneously classified pixel at a certain location, while the intensity function defines the number of errors per unit areas at a certain location. Dividing the intensity $\lambda(Z)$ by its integral over the study area L, produces the density function $f(Z)$ (Diggle and Rowlingson, 1994; Waller and Gotway, 2004).

2.3.2 Density Ratio and Non-parametric Binary Regression: Suppose that we have a number of correct locations and their locations are an independent random sample from the distribution on L with probability density proportional to their intensity $\lambda_1(Z)$. Similarly, we can describe erroneously classified pixels with intensity $\lambda_0(Z)$. Our interest is to estimate the spatial variation of errors in the land cover map. We can use the spatial odds function $d(Z) = \lambda_1(Z)/\lambda_0(Z)$, something analogous with what Kelsall and Diggle (1995a,b), proposed in a spatial epidemiology context. The spatial odds function is constant, $d(Z) = \frac{n_1}{n_0} = d_0$, under the null hypothesis of equal distribution. We could also work with the ratio of densities as an estimation of $d(Z)$ (Bithell, 1990), or the logarithm of this ratio, with the null hypothesis that the function of logarithm of the ratio of the densities, $rd(Z) = log(f_1(Z)/f_0(Z))$, equals to 0.

A test statistic $T = \int_L (d(Z) - d_0)^2 dZ$ has been proposed by Kelsall and Diggle (1995a) to test the null hypothesis of equal distribution of errors and non-errors, using Monte carlo simulations as a test of significance (Kelsall and Diggle, 1995b). In brief, the test is based on computing k values of the test statistic T by randomly re-labeling errors and non-errors, keeping their numbers n_0 and n_1 fixed. The significance (p-value) can then be estimated by the rank of T_0 (computed for the observed data) in the series of the k T values.

Conditional on the whole set of locations, Y_i are independent Bernoulli trials (Diggle and Rowlingson, 1994) with:

$$P(Y_i = 1|Zi) = \pi(Z_i) = \frac{\lambda_1(Z_i)}{\lambda_1(Z_i) + \lambda_0(Z_i)} \tag{2}$$

We can therefore estimate the probability of error in any location following the above and estimating $\lambda_1(Z)$ and $\lambda_0(Z)$ as kernel densities.

A cross-validation method for choosing the bandwidth was devised by Kelsall and Diggle (1995a,b) using Taylor series expansion.Bithell (1990) and Kelsall and Diggle (1995a,b) suggested that the same bandwidth should be chosen for both kernels in order to minimize any error exaggeration at the tails when taking the ratio of the kernels.

2.3.3 Generalized Additive Modeling: When we need to examine spatial variation of errors taking into account covariates, then the use of Generalized Additive Models (GAM) is appropriate (Hastie and Tibshirani, 1990; Diggle, 2006; Elliot et al., 2006).

If there were other factors to include in the modeling an additive logistic model with the following form would be needed:

$$logit(\pi(Z)) = log(\frac{\pi(Z)}{1 - \pi(Z)} = \beta_0 + \sum_{i=1}^{N} \beta_i * g_i(Z) + S(Z) \tag{3}$$

where $\pi(Z)$ represents the probability for a location to be correct (non-error) given its location Z, $g_i(Z)$ represents the covariates (if any) which take into account known factors that influence the status of the location, $S(Z)$ is the smooth factor representing the spatial variation of non-errors (or errors). The model implemented here does not use any covariates (so only the intercept and the $S(Z)$ terms are needed in the above equation). In particular, according to Diggle (2006), $exp(S(Z))$ denotes the residual odds ratio of the correct/error status controlling for the rest known risk factors. Kelsall and Diggle (1998) used a Kernel estimator as the $S(Z)$ function with an adjusted bandwidth according to a cross-validation criterion. However, in this case $S(Z)$ was chosen to be a thin plate spline function (Wood, 2006) as it was easier to implement. This is not expected to have a significant effect in the model as the choice of smooth function generally does not change dramatically the results (except for cases where there are specific reasons to choose a particular smooth function) (Diggle, 2003). A final point that should be made here is that the null hypothesis is that the smooth factor $S(Z)$ is constant rather than $\pi(Z)$ (Diggle, 2006).

2.4 Change detection under uncertainty

Modeling results will provide us with information related to the distribution of errors. If the errors are equally distributed to the study area and their total percentage is not too high (e.g. within 10%) then we can proceed to post-classification change detection without any further processing. But if we have proof that there is spatial variation in the errors (e.g. factor $S(Z)$ is significant), then we need to take this into account.

One way of proceeding would be to identify the areas where the probability of errors are high and try to correct them either with extra samples and reclassification or with some auxiliary data. If this is not possible then we could proceed to change detection attaching a degree of confidence in our estimates of change. Currently this is a matter of ongoing research and here a visualization of the local variation of errors is presented (see figure 6). In addition, a box-plot of land cover changes against the variation of non-errors/errors is also presented in the results in order to evaluate the performance of change detection estimates (see figure 7).

3 RESULTS AND DISCUSSION

A summary of the GAM fitting results are presented in table 1. As we can see, in all models the spatial factor $S(Z) = S(X, Y)$, which is a smooth function of location variables X and Y, is significant. This suggests that there is a significant spatial variation

in the non-error/error on the locations in the area. The UBRE criterion was used for smoothing parameter estimation for all binomial models, and as we can see from the estimated degree of freedoms the models selected are relatively complex. As Wood (2006) explains model checking with binary data is not straightforward. Often the use of simulation is needed in order to compare the residuals empirical distribution function with the distributions of well (according to assumptions) behaved residuals. In our case this is even more difficult if we take into account the amount of (spatial) data involved and the time needed to simulate enough datasets. In addition, conventional residual plots will not give us information regarding the autocorrelation of residuals. Variograms were used in order to check for possible spatial dependence in the residuals (see figure 1). The percentage of deviance explained is also shown in table 1, indicating that there are other factors, not included here that influence the probability of erroneous classification. This is true for any classified image as there are numerous factors that could influence the success of the classification. However the aim here was to identify the spatial variation in order to make informed decisions for further processing or usability of the change detection results.

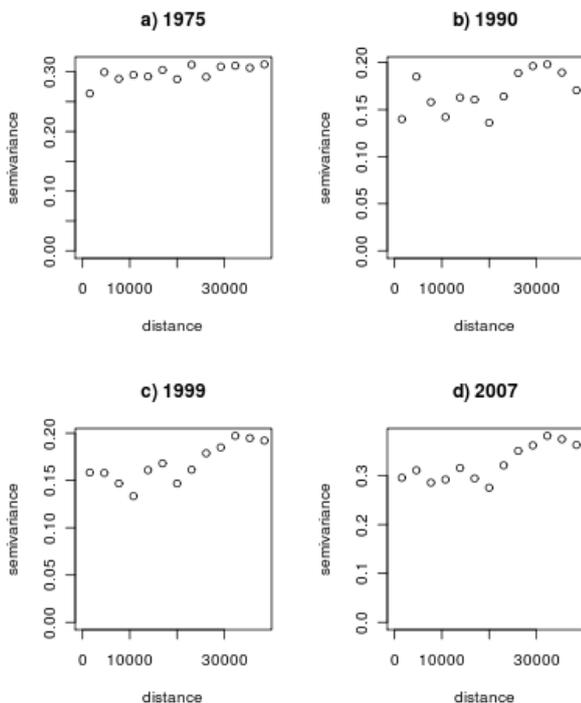|	1975 Model	1990 Model	1999 Model	2007 Model
Intercept	14.171	76.03	52.20	29.105
(Std.Err)	2.181	16.83	12.93	6.448
(p-value)	8.13e-11	6.27e-06	5.44e-05	6.37e-06
s(X,Y)(p-value)	8.38e-13	0.000531	2.32e-06	1.41e-06
edf	143	98.58	77.05	163.7
Dev.expl.	57.1%	66%	51.4%	54.1%
UBRE score	-0.58499	-0.72329	-0.76853	-0.59905
n	2647	2605	2682	3029

Table 1: Model results

Figure 1: Variograms of the deviance residuals for each image

Model predicted probabilities for the error status of each pixel (at the image's resolution) are shown in figures 2,3,4,5.

The results shown in figures 2-5 were for each classified image separately. Although this is extremely useful itself, an estimation is needed for the propagation of the error should a change detection map is produced. Work on this issue is still under
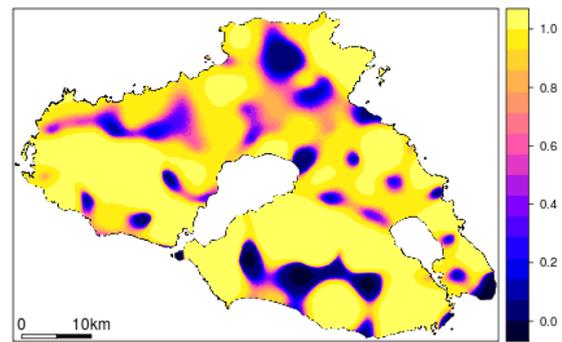

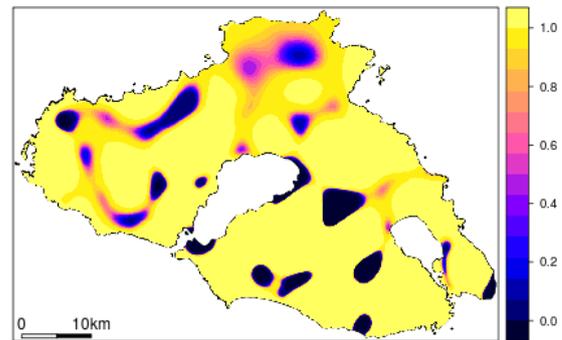Figure 2: Probability of pixels being correctly classified (1975)

Figure 3: Probability of pixels being correctly classified (1990)
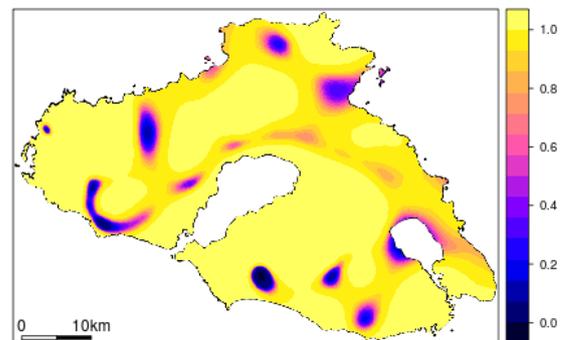

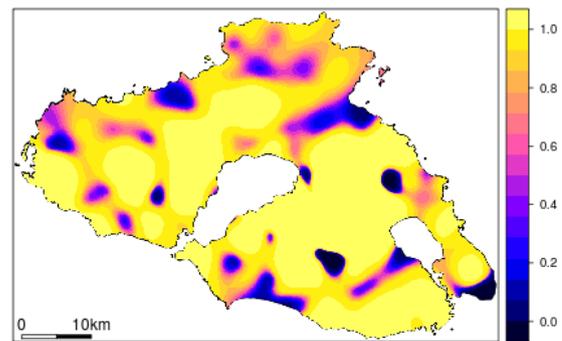Figure 4: Probability of pixels being correctly classified (1999)

Figure 5: Probability of pixels being correctly classified (2007)

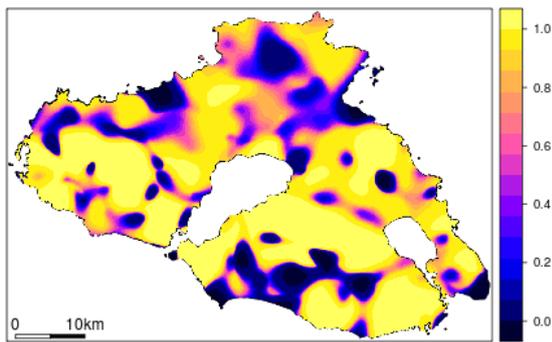progress, however a simple illustration can be seen below where

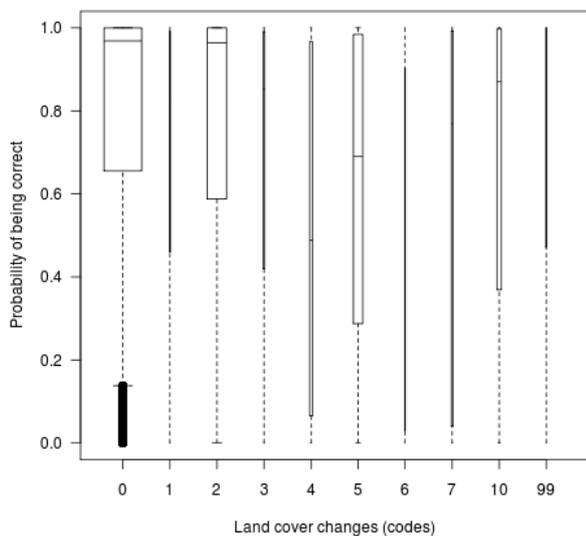Figure 6: Error propagation for 1975 and 2007 images (units are probabilities of being correct)

Figure 7: Boxplot of land use changes vs probabilities of being classified correctly 0:No change, 1:Bare Land to other, 2:Garrigue losses, 3:Other crops losses, 4:Maquies losses, 5:Olives losses, 6:Chestnuts losses, 7:Pines losses, 10:Olives gains, 99:Not possible. Box-plot width indicates pixel counts

the maps were considered as independent and the product of their expected values was used to depict the combined probability of non-error/error and its spatial variation for the change detection map (see figure 6). Significance estimates are also needed here but they are not available at the moment.

As a final result, a visualization/evaluation of the performance of the change detection statistics can be produced in the form of a box-plot of land use changes vs probabilities of change being identified correctly (see figure 7). As we can see from this plot, the easily distinguished categories such as changes of the phryganic vegetation are above 60% (at least the 75% of their distribution). Categories such as olive grove changes (losses:5 and gains:10) having probabilities of being correctly identified changes as low as 40% or even lower. This is mainly due to the confusion of their spectral signatures with maquis (that include abandoned oak cultivations). There is an opportunity here to assess visually the quality of the change detection estimates.

4 CONCLUSIONS AND FUTURE WORK

From the results shown above we can see that it is possible to use ground truth data and generalized additive modeling to assess the spatial variation of non-errors/errors in land cover map. We can also project the error propagation to the change detection map, evaluating the probability to observe a true change. There are still many challenges on the issue discussed and ongoing work now is concentrating in modeling error propagation through the multitemporal imagery and estimating significance of the final error map.

References

Bailey, T. and Gatrell, A., 1995. Interactive Spatial Data Analysis. Longman.

Bithell, J., 1990. An application of density estimation to geographical epidemiology. Statistics in Medicine 9, pp. 691–701.

Bivand, R., 2010. spgrass6: Interface between GRASS 6 and R. R package version 0.6-16.

Bivand, R., Pebesma, E. and Gomez-Rubio, V., 2008. Applied Spatial Data Analysis with R. Springer.

Crosetto, M., Moreno Ruiz, J. A. and Crippa, B., 2001. Uncertainty propagation in models driven by remotely sensed data. Remote Sensing of Environment 76(3), pp. 373–385.

de Bruin, S., 2000. Predicting the areal extent of land-cover types using classified imagery and geostatistics. Remote Sensing of Environment 74(3), pp. 387–396.

Diggle, P., 2003. Statistical Analysis of Spatial Point Patterns. 2nd edn, Hodder Arnold.

Diggle, P., 2006. Spatial Epidemiology: Methods and Applications. (reprint) edn, Oxford University Press, chapter Overview of statistical mehtods for disease mapping and its relationship to cluster detection, pp. 87–103.

Diggle, P. and Rowlingson, B., 1994. A conditional approach to point process modelling of raised incidence. Journal of Royal Statistical Society, Series A 157, pp. 433–440.

Elliot, P., Wakefield, J. C., Best, N. G. and Briggs, D. J., 2006. Spatial Epidemiology - Methods and Applications. (reprint) edn, Oxford University Press.

Gatsis, I. and Koukoulas, S., 2009. Human induced land cover/use changes in lesvos island (greece), during the 1984-2007 period. In: Proceedings of the 11th International Conference on Environmental Science and Technology, Chania, Crete, Greece.

Gatsis, I., Koukoulas, S., Vafeidis, A. and Gkoltsiou, K., 2007. Monitoring and mapping of land cover/use changes in an agricultural and natural environment, using multitemporal satellite data and gis (lesvos island, greece). In: CEST 2007 - 10th International Conference on Environmental Science and Technology, Kos Island, Greece.

Gatsis, I., Koukoulas, S., Vafeidis, A., Lagoudakis, E. and Gkoltsiou, K., 2006. Monitoring and mapping of land cover/use changes in an agricultural and natural environment, using multitemporal satellite data and gis (lesvos island, greece). In: Proceedings of RSPSoc Annual Meeting, University of Cambridge.

Giourga, C., Loumou, A., Tsevreni, I. and Vergou, A., 2008. Assessing the sustainability factors of traditional olive groves on lesvos island, greece (sustainability and traditional cultivation). GeoJournal 73(2), pp. 149–159.

Hastie, T. and Tibshirani, R., 1990. Generalised Additive Models. Chapman & Hall (London).

Kelsall, J. and Diggle, P., 1995a. Kernel estimation of relative risk. Bernoulli 1, pp. 3–16.

Kelsall, J. and Diggle, P., 1995b. Non-parametric estimation of spatial variation in relative risk. Statistics in Medicine 14, pp. 2335–2342.

Kelsall, J. and Diggle, P., 1998. Spatial variation in risk: a nonparametric binary regression approach. Applied Statistics 47, pp. 559–573.

Koukoulas, S. and Blackburn, G., 2001. Introducing new indices for accuracy evaluation of classified images representing semi-natural woodland environments. Photogrammetric Engineering and Remote Sensing 67, pp. 499–510.

Kyriakidis, P. and Dungan, J., 2001. A geostatistical approach for mapping thematic classification accuracy and evaluating the impact of inaccurate spatial data on ecological model predictions. Environmental and Ecological Statistics 8, pp. 311–330.

Lewin-Koh, N. J., Bivand, R., contributions by Edzer J. Pebesma, Archer, E., Baddeley, A., Bibiko, H.-J., Dray, S., Forrest, D., Friendly, M., Giraudoux, P., Golicher, D., Rubio, V. G., Hausmann, P., Jagger, T., Luque, S. P., MacQueen, D., Niccolai, A., Short, T. and Stabler, B., 2010. maptools: Tools for reading and handling spatial objects. R package version 0.7-33.

Neteler, M. and Mitasova, H., 2008. Open Source GIS: a GRASS GIS Approach. Springer, New York.

R Development Core Team, 2009. R: A Language and Environment for Statistical Computing. R Foundation for Statistical Computing, Vienna, Austria. ISBN 3-900051-07-0.

Rowlingson, B., Diggle, P., adapted, packaged for R by Roger Bivand, pcp functions by Giovanni Petris and goodness of fit by Stephen Eglen, 2009. splancs: Spatial and Space-Time Point Pattern Analysis. R package version 2.01-25.

Silverman, B., 1986. Density estimation for statistics and data analysis. Chapman and Hall, London.

van Oort, P., 2007. Interpreting the change detection error matrix. Remote Sensing of Environment 108(1), pp. 1–8.

Waller, L. and Gotway, C., 2004. Applied Spatial Statistics for Public Health Data. Wiley.

Wang, M. and Howarth, P. J., 1993. Modeling errors in remote sensing image classification. Remote Sensing of Environment 45(3), pp. 261–271.

Wood, S. N., 2006. Generalized Additive Models - An Introduction with R. Chapman & Hall/CRC.